applied sciences

Article

Proactive Braking Control System for Collision Avoidance during Right Turns with Occluded Vision at an Intersection

Sota Aoki [1,*], Yohei Fujinami [1], Pongsathorn Raksincharoensak [1] and Roman Henze [2]

[1] Department of Mechanical Systems Engineering, Tokyo University of Agriculture and Technology, 2-24-16 Naka-cho, Tokyo 184-8588, Japan; y-fujinami@go.tuat.ac.jp (Y.F.); pong@cc.tuat.ac.jp (P.R.)
[2] Institute of Automotive Engineering, Technical University of Braunschweig, Hans-Sommer Strasse 4, 38106 Braunschweig, Germany; r.henze@tu-bs.de
* Correspondence: s229710t@st.go.tuat.ac.jp; Tel.: +81-42-388-7397

Abstract: This paper describes the development of an Advanced Driver Assistance System (ADAS) which will allow drivers to avoid collisions with an oncoming vehicle from an occluded area when turning right at intersections in left-hand traffic. Connected vehicles, in coordination with infrastructure, represent one of the commercialized ADAS technologies for collision avoidance. However, the coverage of the ADAS will be limited to designated intersections only, as communication equipment needs to be installed in both the vehicle and infrastructure to enable the assistance. This paper proposes an ADAS using on-board sensors, independent of infrastructure facilities, to control the vehicle velocity to avoid collisions. Most current intersection assistance, by using an Autonomous Emergency Braking System (AEBS), allows the driver to avoid a collision with oncoming vehicles when there is clear vision without occlusion. However, many accidents occur when the vehicle detects the oncoming vehicle too late because of occlusion in the intersection, such as a vehicle in the opposite lane. This system calculates the hazardous speed criteria of the ego vehicle, which might result in a high risk of collision when darting out occurs, and provides speed control assistance to allow the driver to escape from the hazardous speed region. The simulation results reveal that the proposed system effectively reduces the possibility of collisions compared to conventional AEBS.

Keywords: ADAS; intersection; intersection right turn; collision avoidance; risk prediction; dilemma zone

check for updates

Citation: Aoki, S.; Fujinami, Y.; Raksincharoensak, P.; Henze, R. Proactive Braking Control System for Collision Avoidance during Right Turns with Occluded Vision at an Intersection. *Appl. Sci.* **2024**, *14*, 2661. https://doi.org/10.3390/app14062661

Academic Editors: Mauro Dell'Orco and Mario Marinelli

Received: 9 February 2024
Revised: 4 March 2024
Accepted: 11 March 2024
Published: 21 March 2024

1. Introduction

In recent years, the number of traffic accidents and fatalities in Japan has been decreasing due to the improvement of the road traffic environment, as well as the spread of Advanced Driver Assistance Systems (ADASs) such as the Autonomous Emergency Braking System (AEBS). However, the number of accidents remains at a high level. In particular, more than half of all fatalities and injurious traffic accidents occur near intersections [1]. Furthermore, when we look at accidents within intersections, right-turn accidents have accounted for the highest percentage of accidents at intersections involving four-wheeled vehicles in left-hand traffic in Japan, comprising about 40% [2]. Therefore, there is a social need to develop ADAS to prevent accidents occurring when drivers make right turns, and much research on this topic has been conducted in recent years.

Sander conducted a simulation study of a left turn across a path with traffic from the oncoming direction in right-hand traffic to show the effectiveness of the turning vehicle's AEBS [3,4]. Furthermore, according to literature survey, there are a number of studies attempting to develop a vehicle control algorithm for the purpose of autonomous collision avoidance in left turn/right turn across path scenarios [5–12]. On the other hand, collision avoidance methods utilizing connected vehicle technologies are also being developed for the same scenarios [13–17]. In addition, in order to enhance these collision avoidance systems, many analyses on accident causal factors are being conducted using naturalistic driving data, driving simulator experiments, and simulations [18–23].

In the right-turning scenes of left-hand traffic in countries like Japan, the risk of accidents is particularly high in critical scenarios, e.g., when a vehicle suddenly darts out from a blind area with a short time margin to collision, as shown in Figure 1. This is because the driver and AEBS may not have enough time to react or a sufficient braking distance to avoid a collision with the darting-out object in time. Connected vehicles in coordination with infrastructure have been commercialized as ADAS technologies for this situation, but they cannot provide assistance unless communication equipment is installed in both the vehicle and the infrastructure. Therefore, the coverage of the ADAS will be limited only to the designated intersections. In response to this disadvantage, in a previous study, the authors' research group proposed a system in which, when on-board sensors recognize a blind area, the vehicle decelerates in advance to a speed at which AEBS can avoid the collision after detecting the darting out [24]. However, because the system assumes the activation of AEBS, the rear-end collision risk with a following vehicle arises when the ego vehicle suddenly decelerates. Furthermore, since the system previously proposed in [24] attempts to pass through the intersection unless the on-board sensor detects darting-out, a collision may be unavoidable if the object detection is late.

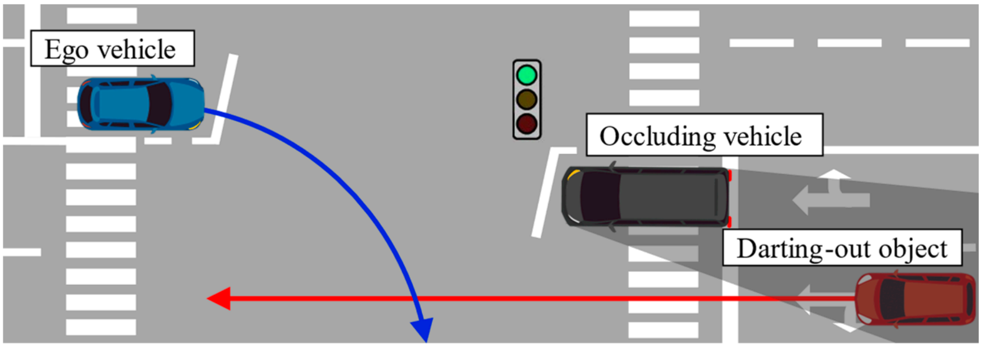

Figure 1. Darting-out scenario at intersection right turning.

Therefore, this study aims to develop an enhanced ADAS to avoid collisions with oncoming vehicles darting out from a blind area when drivers are making a right turn at an intersection without using infrastructure coordination facilities and AEBS. In this paper, we focus on an intersection right-turn situation where an object darts out from the blind area of an oncoming vehicle stopped near the intersection entrance, as shown in Figure 1. Our proposed ADAS, the proactive braking system (PBS), is a system that provides proactive braking assistance to reduce the risk of collision even before darting-out occurs. To solve the problems of the previous system, the new system basically uses only mild deceleration maneuvers up to 0.3 g without emergency braking, even if an object darts out. Furthermore, by predicting high-risk conditions in advance and stopping the vehicle, collisions are avoided even in critical situations.

First, in Section 2, the two hazardous speed criteria of the ego vehicle to define the target speed for PBS are described. The first speed criterion is defined as the speed at which the ego vehicle can safely stop when the darting-out occurs, and the second is defined as the speed at which the ego vehicle can escape the intersection before making contact with the darting-out object. Next, in Section 3, PBS provides speed control assistance to prevent the vehicle from entering the hazardous speed region between these speed criteria. Finally, in Section 4, simulations are performed to verify the effectiveness of the proposed PBS for various darting-out conditions and compared the collision avoidance performance between the proposed method and driver assistance systems from the conventional technology and the previous study.

2. Risk Prediction under Occluded Vision for Proactive Braking Control Design

2.1. Design Concept

Figure 2 shows a schematic overview of the system. The system predicts the trajectory of the vehicle using a Triclothoidal curve [25] based on the vehicle status, intersection map information, and driver maneuver. The Triclothoidal curve is a curve that consists of three clothoid curves connected without discontinuities in curvature. Using the predicted trajectory and the positioning information on the occluding vehicle detected by on-board sensors, PBS calculates the hazardous speed criteria of the ego vehicle that is at high collision risk in a predicted future horizon of a certain number of seconds ahead. The derivation of this speed criteria is based on the idea of a dilemma zone [26]. The dilemma zone, in the context of traffic, generally refers to the range of dangerous vehicle speed for vehicles approaching an intersection when the traffic light changes to yellow. If the vehicle speed is within the dilemma zone, it is too far from the intersection to completely pass through it before the red light begins. On the other hand, the vehicle is too close to the intersection to stop safely or comfortably. Similarly, in the right-turn scenario with the blind area of the oncoming vehicle, there is a speed range in which safe collision avoidance is not possible. Therefore, in this study, the dilemma zone is applied to the right-turn scene to obtain the "right-turn dilemma zone". To help the vehicle escape from the right-turn dilemma zone, the system calculates the desired acceleration and provides speed assistance.

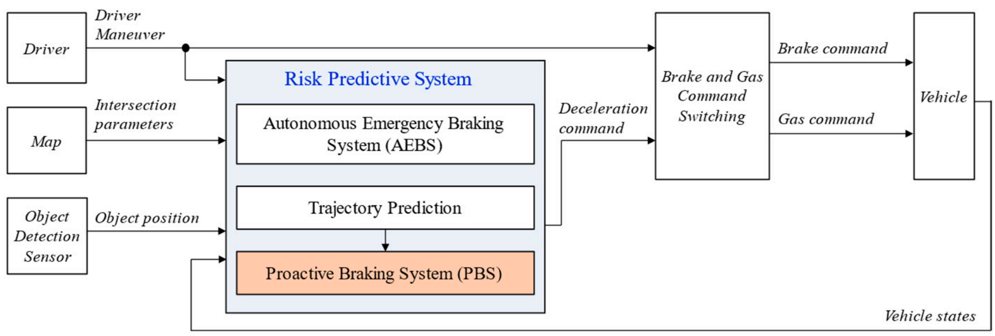

Figure 2. Schematic overview of proposed proactive braking system for intersection right turn.

2.2. Quantification of Hazardous Speed Region for Right Turn

Depending on the scenario in which the vehicle darts out, the system executes one of the following two patterns of action. (a) Collision avoidance by mild and moderate deceleration. (b) The ego vehicle passes in front of the darting-out object. This paper defines the maximum velocity satisfying the condition (a) as the safe velocity V_{safe} and the minimum velocity satisfying the condition (b) as the escapable velocity V_{esc}, as shown in Figure 3. The safe velocity V_{safe} is calculated based on the method proposed by Fujinami et al. [24].

Figure 3. Driving according to hazardous speed criteria V_{safe} and V_{esc}. (**a**) Deceleration in case of condition; (**b**) turning right in case of condition.

In this research, there is an on-board sensor installed on the right-front edge of the ego vehicle. The on-board sensor is assumed to be a LIDAR, which provides information on the object's position and speed after detection. When the on-board sensor detects an occluding vehicle, the system predicts the conflict area by calculating the predicted trajectories of the darting-out object and the ego vehicle. First, a Triclothoidal curve is used to predict the trajectory of the ego vehicle's rear-axle center point during a right turn (vehicle-fixed coordinates (x, y) and the relative yaw angle from the current ego vehicle yaw angle at each coordinate), as shown in Figure 4. Based on the predicted trajectory of the center point of the rear axle and the size of the vehicle, the trajectory of the entire vehicle is predicted. Next, in order to predict the risk before the darting out actually occurs, a virtual darting-out object is assumed to dart out from the blind area. The virtual darting-out object is defined as traveling straight in the center of the oncoming lane at a constant speed. The conflict area is calculated by finding the area where the predicted trajectory of the entire ego vehicle overlaps with the defined trajectory of the virtual darting-out object. The stop position when the ego vehicle avoids a collision is defined as the position where the on-board sensor can see through the blind driving corridor at the same time that there is a margin of distance to the conflict area.

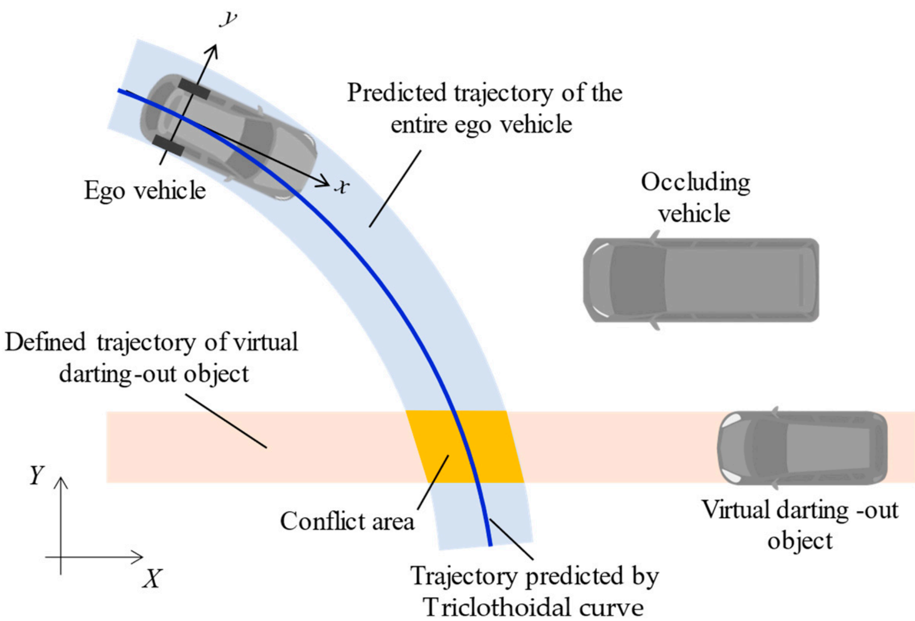

Figure 4. Predicted trajectory of ego vehicle and defined trajectory of virtual darting-out object.

Equation (1) expresses the safe velocity V_{safe} at which the vehicle can smoothly decelerate when darting out occurs and stop in front of the predicted conflict area where the sensor can see through the blind driving corridor.

$$V_{safe}(t) = a_b T_d + \sqrt{(a_b T_d)^2 - 2a_b D_{stop}(t)} \quad (1)$$

where T_d is the system activation delay time and a_b is the acceleration for mild deceleration. In addition, as shown in Figure 5, D_{stop} is the distance on the predicted trajectory from the ego-vehicle current position to the stop position. The safe speed V_{safe} is the speed criterion for stopping by decelerating at a_b. Therefore, if the vehicle speed is so high that the vehicle cannot stop even if it continues to decelerate with acceleration a_b when entering an intersection, AEBS will be activated to take over the braking maneuver in order to avoid a collision.

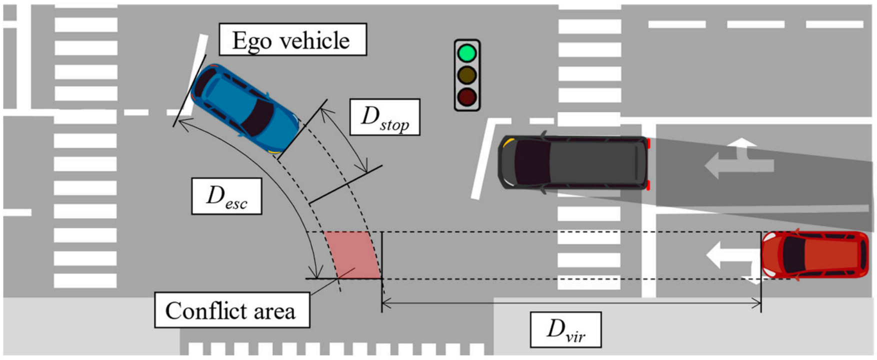

Figure 5. Definitions of the distances for risk prediction calculation.

In the oncoming corridor, the time T_{vir} from when the on-board sensor recognizes the darting out until the object reaches the conflict area is as follows:

$$T_{vir}(t) = \frac{D_{vir}(t)}{V_{vir}} \tag{2}$$

where D_{vir} is the distance from the darting-out point to the conflict area and V_{vir} is the assumed virtual velocity of the darting-out object.

Equation (4), derived from Equation (3), is the minimum velocity V_{esc} at which the vehicle can escape the conflict area before contact with the darting-out object while maintaining the current velocity.

$$V_{esc}(t) = \frac{D_{esc}(t) - V_{esc}(t)T_d}{T_{vir}(t) - PET - T_d} \tag{3}$$

$$V_{esc}(t) = \frac{D_{esc}(t)}{T_{vir}(t) - PET} \tag{4}$$

where D_{esc} is the distance on the predicted trajectory from the vehicle's current position to the position of escaping the conflict area and PET [27] (Post Encroachment Time) is the margin time between when the ego vehicle escapes the conflict area and when the darting-out object reaches it. From the above, V_{safe} and V_{esc} can be calculated by assuming the object darts out with an assumed velocity of V_{vir} or under. Figure 6 shows the schematic images of hazard velocity curves V_{safe} and V_{esc}. The shaded area between V_{safe} and V_{esc} in Figure 6 is set as the right-turn dilemma zone. If the vehicle velocity is within the dilemma zone at the time of darting out, the vehicle cannot avoid a collision by the designated moderate deceleration, nor can it maintain its speed and pass the conflict area before making contact with the darting-out object. Therefore, the vehicle is in a hazardous speed region.

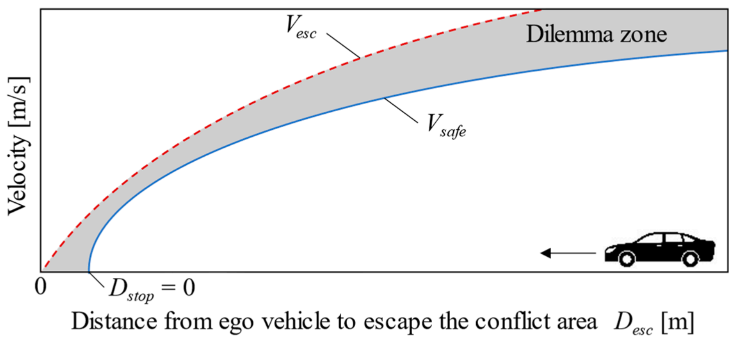

Figure 6. Schematic images of the dilemma zone and hazard velocity curves V_{safe} and V_{esc}.

3. Collision Risk Avoidance Algorithm

3.1. Judgment of Driving Behavior by PBS

The flowchart of this system activation is shown in Figure 7. When the ego vehicle heads to an intersection, the following triggers activate the system: the driver intends to make a right turn at the intersection with the turning indicator, the on-board sensor detects an occluding vehicle on the oncoming lane, and there is a driving corridor behind the occluding vehicle where an object can dart out. In order to safely avoid a collision when darting out occurs, the vehicle velocity should be controlled in advance before the darting out occurs so that the vehicle does not enter the right-turn dilemma zone. To make this possible, when the system is activated, it calculates V_{safe} and V_{esc} at the point where the ego vehicle has traveled at the current velocity for the prediction time of T_p seconds by predicting darting-out. If the calculation results in $V_{esc} > V_{safe}$, a dilemma zone exists. Therefore, PBS decelerates the vehicle to prevent it exceeding V_{safe}. As the vehicle traveling straight has priority over the vehicle turning right at intersections, the ego vehicle basically travels at V_{safe} or under until the visibility improves. Additionally, if $V_{safe} = 0$, the system will stop the vehicle. The same deceleration assistance is also provided when the vehicle velocity is lower than V_{esc}.

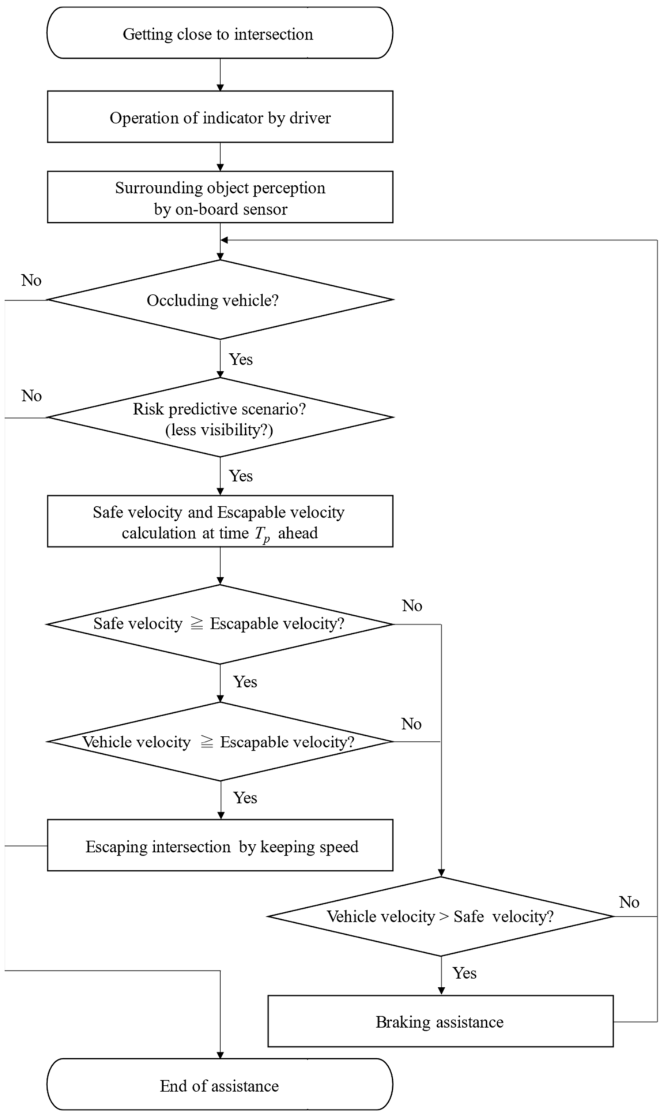

Figure 7. Flowchart of the system activation.

Conversely, if $V_{safe} \geq V_{esc}$ and the vehicle velocity is higher than V_{esc}, there is no dilemma zone and the ego vehicle can escape the intersection while maintaining the current velocity.

3.2. Sensor Position and Assistance after Stopping

After the vehicle has stopped, the on-board sensor detects an approaching oncoming vehicle in the driver's blind driving corridor and informs the driver about its existence to assist in restarting the vehicle. For this purpose, the on-board sensor for PBS is mounted on the right front edge of the vehicle. Figure 8 shows the mounting positions of the on-board sensor and the visibility of the sensors when the vehicle is stopped. Compared to the conventional mounting position, by setting it at the right front edge, the amount of protrusion from the left side of the occluding vehicle is reduced when the ego vehicle is stopping. Then, the target stop position is the position in which it is possible to both avoid collisions safely and see through the object's driving corridor. The proposed driver assistance system requires a sensor that is mounted to the right front edge. However, the sensor is assumed to be one of the sensors that can be utilized for other ADAS at intersections such as cross-traffic detection sensors. Therefore, sensors are installed on both sides of the vehicle to provide assistance when turning left as well. Furthermore, the sensor in the conventional mounting position at the center is used for other ADAS functions such as Adaptive Cruise Control (ACC), so both sensors in the conventional position and the corner sensors are actually mounted.

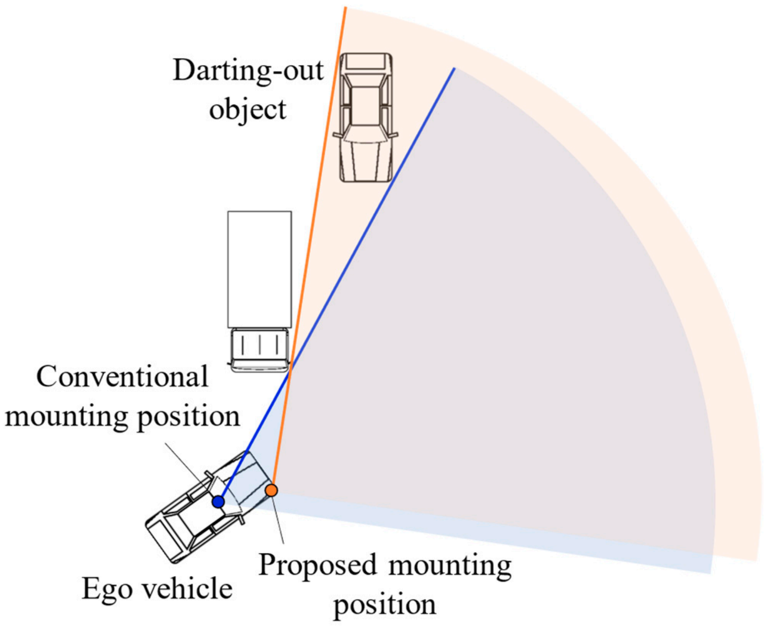

Figure 8. On-board sensor positions and the visibility when the ego vehicle is stopped.

4. System Verification with Full-Vehicle Simulation

This section describes the simulation and analysis to evaluate the collision risk-avoidance performance of the PBS. We used IPG CarMaker® Ver. 9.1.1 software for the full-vehicle simulations. In this simulation, we compared vehicles equipped with PBS and AEBS versus those equipped with AEBS only.

4.1. Autonomous Emergency Braking System

After detecting a darting out, AEBS predicts the trajectory of the ego vehicle and the darting-out object using the same method as PBS. Figure 9 is a diagram of the relationship between the ego vehicle and the darting-out object. The intersection of the two trajectories is the conflict area. The time until the ego vehicle enters the conflict area and the time until it exits it are as follows:

$$T_{ego\_in}(t) = \frac{D_{ego\_in}(t)}{V_{ego}(t)} \quad (5)$$

$$T_{ego\_out}(t) = \frac{D_{ego\_out}(t)}{V_{ego}(t)} \quad (6)$$

where D_{ego_in} indicates the distance until the ego vehicle enters the conflict area and D_{ego_out} is the distance until it exits. Similarly, the time until the object enters the conflict area and the time until it exits are as follows:

$$T_{obj\_in}(t) = \frac{D_{obj\_in}(t)}{V_{obj}(t)} \quad (7)$$

$$T_{obj\_out}(t) = \frac{D_{obj\_out}(t)}{V_{obj}(t)} \quad (8)$$

where D_{obj_in} indicates the distance until the object enters the conflict area, D_{obj_out} is the distance until it exits, and V_{obj} is the velocity of the darting-out object. AEBS decelerates the vehicle with 100% brake pedal stroke when the system determines that a collision is about to occur if the ego vehicle and the darting-out object maintain their current velocity. The AEBS activating condition is as follows:

$$(T_{ego\_in}(t) - T_{obj\_out}(t) < 0.5) \wedge (T_{obj\_in}(t) - T_{ego\_out}(t) < 0.5) \wedge (T_{ego\_in}(t) \leq 1.4) \quad (9)$$

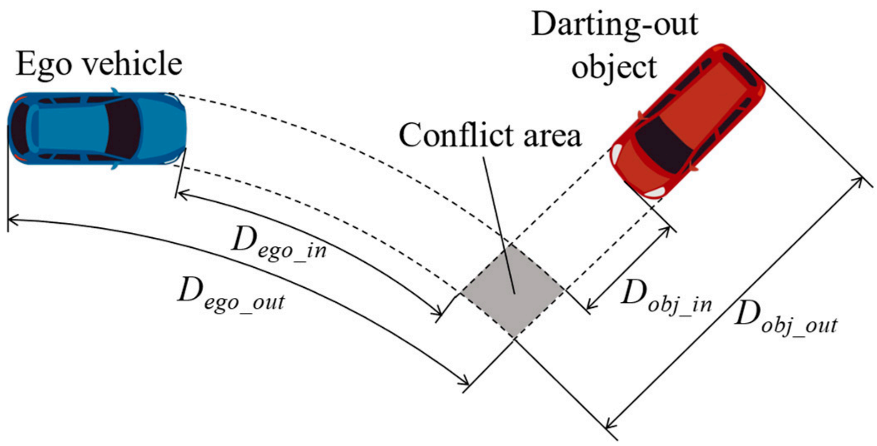

Figure 9. Geometric relationship between ego vehicle and darting-out object.

Since the objective of this research is collision avoidance without emergency braking, the AEBS is a supplementary function for cases where PBS cannot decelerate sufficiently (e.g., when the darting-out velocity is much higher than predicted). Therefore, although the design of AEBS was described, its design is not the focus of this study.

4.2. Simulation Conditions

Intersection geometry is one of the key parameters in analyses focused on traffic safety at intersections. Perri et al. [28] stated that intersection geometry and intersection type influence driver behaviour at unsignalized intersections. This study focuses on a typical intersection geometry in Japan as a representative case, as shown in Figure 10a,b. As shown in the figures, the target road is a flat, right-angled, urban intersection where there is no longitudinal slope. The traffic lights are assumed to be in green status in both directions (meaning the ego vehicle could turn right and oncoming vehicles could continue straight ahead). The simulations were conducted in an environment where there were no channelizing islands or median strips, and only oncoming vehicles had a blind area.

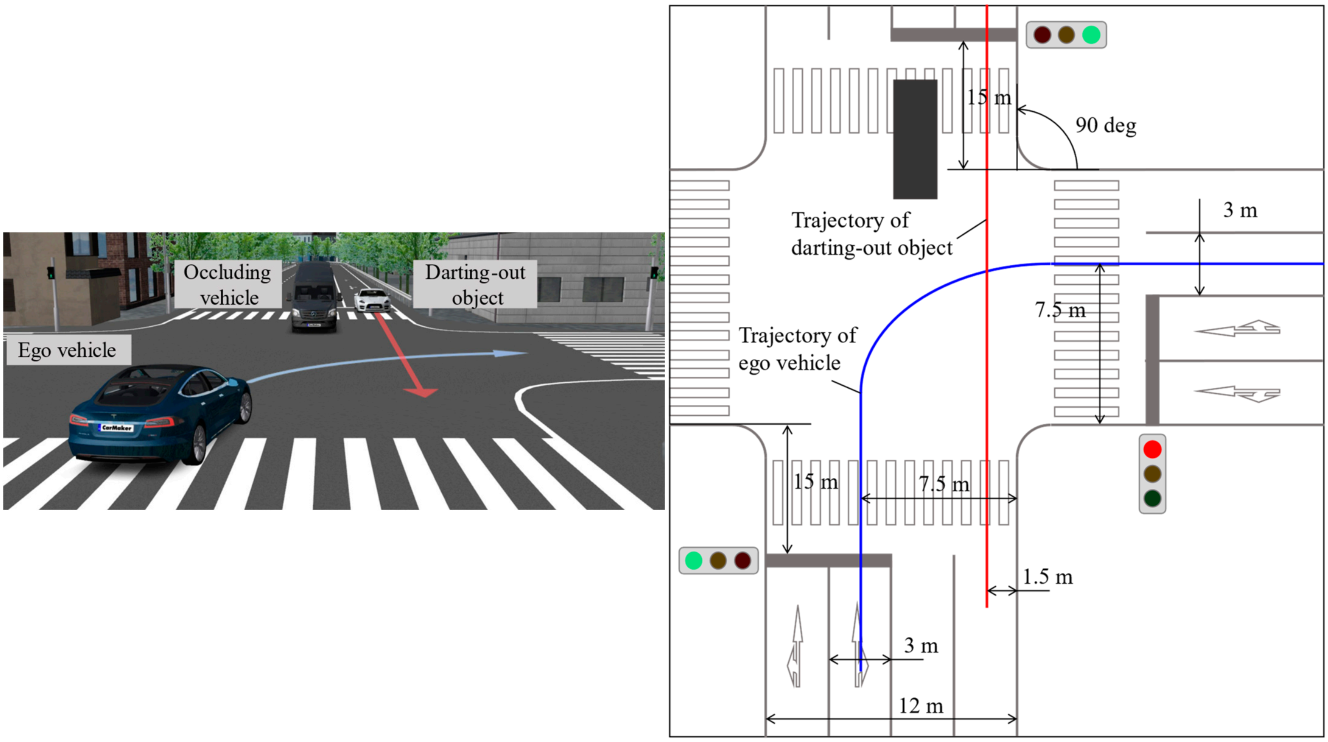

(**a**) (**b**)

Figure 10. Intersection right-turn scene using full-vehicle simulation. (**a**) Object darting-out scene; (**b**) geometry of the target intersection.

In the target intersection, an oncoming four-wheeled vehicle darted out from the blind area of another stopped oncoming four-wheeled vehicle that was waiting to turn right when the ego vehicle turned right. After accelerating to an initial velocity of 40 km/h, the driver of the ego vehicle entered the intersection without operating the gas pedal and brake pedal. Therefore, the driver only operated the steering wheel during the right turn, and the vehicle velocity was controlled only when the speed assist system intervened. As shown in Figure 11, the on-board sensor was mounted on the right front edge of the ego vehicle, with detection distance R_{sensor} = 120 m and FOV = 70°.

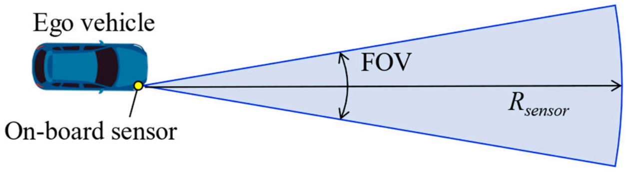

Figure 11. Definition of sensor detection range and FOV.

It is assumed in the simulation that the sensor is able to recognize a darting-out vehicle with no delay time when the entire body of the target vehicle becomes visible. The detailed requirements for on-board sensors to detect oncoming vehicles in the real world (e.g., detection distance and azimuth) are presented by Scanlon et al. [29]. In order to fairly compare the collision avoidance performance among various simulation conditions, the paths of the ego vehicle and the oncoming vehicle were strictly fixed in all conditions in the simulation. And the darting-out object entered the intersection at a constant speed while maintaining the lateral distance from the occluding vehicle D_{obj_lat} = 1.2 m, as shown in

Figure 12. The occluding vehicle stopped at a distance from the trajectory of the ego vehicle D_{occ} = 7 m.

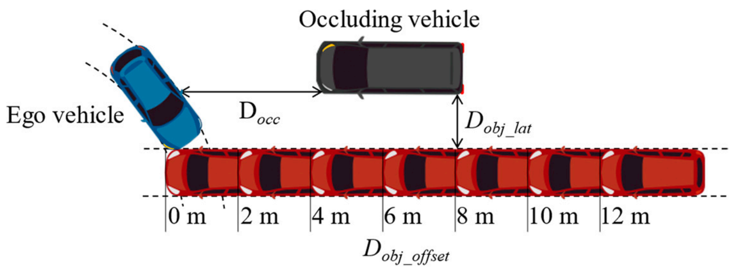

Figure 12. Definition of vehicle position conditions.

To evaluate the effectiveness of the system in various darting-out conditions, two scenario parameters were varied repeatedly. The first parameter was the velocity of the darting-out object V_{obj} and the second was the offset position of the darting-out object D_{obj_offset}. Simulations were performed under 441 different conditions, varying V_{obj} from 30 to 50 km/h and D_{obj_offset} from 0 to 40 m. As shown in Figure 12, D_{obj_offset} = 0 m was the position in which the ego vehicle and object would collide if they did not change their initial velocities and take any avoidance actions. Therefore, the initial position of the darting-out object is set so that a collision or near-miss situation between the ego vehicle and the object at the intersection will occur if the ego vehicle does not brake. The collision risk avoidance performances of vehicles equipped with the PBS and AEBS, or with AEBS only, were evaluated by comparing the presence/absence of collisions as well as the distance to the closest point of approach (DCPA) between the ego vehicle and the darting-out object under each condition. The values of the various parameters are shown in Table 1. Then, the speed limit at the intersection was set at 50 km/h and V_{vir} was also set to the same value.

Table 1. Driving condition parameters.

Definition	Symbol	Value	Unit
Acc. for mild deceleration	a_b	−2.94	m/s^2
System activation delay time	T_d	0.1	s
Prediction time	T_p	2.0	s
Post Encroachment Time	PET	1.0	s
Virtual darting-out velocity	V_{vir}	50	km/h

4.3. Results and Discussions

Figure 13 shows examples of the time history of vehicle motion (V_{obj} = 50 km/h, D_{obj_offset} = 16 m). It also shows the simulation results of velocity, acceleration, and system brake pedal stroke for AEBS only and for both PBS and AEBS cases, respectively. The red dotted line in Figure 13a indicates when the collision occurred, and the green dotted line in Figure 13b indicates the safe velocity V_{safe}. Figure 13a,b show that the vehicle initially decelerated the vehicle at about −0.3 m/s^2 for both systems because the driver did not operate the pedals. Regarding the system response, Figure 13a shows that AEBS increased the brake pedal stroke from 0% to 100% after detecting a darting out, and the vehicle suddenly decelerated to a stop. However, since the ego vehicle entered the object's driving corridor, the collision could not be avoided. On the other hand, as shown in Figure 13b, the PBS decelerated the vehicle in advance so that the vehicle velocity became lower than the safe velocity. Therefore, when darting out occurred, the vehicle was able to stop before entering the conflict area without activating AEBS, and the collision did not occur.

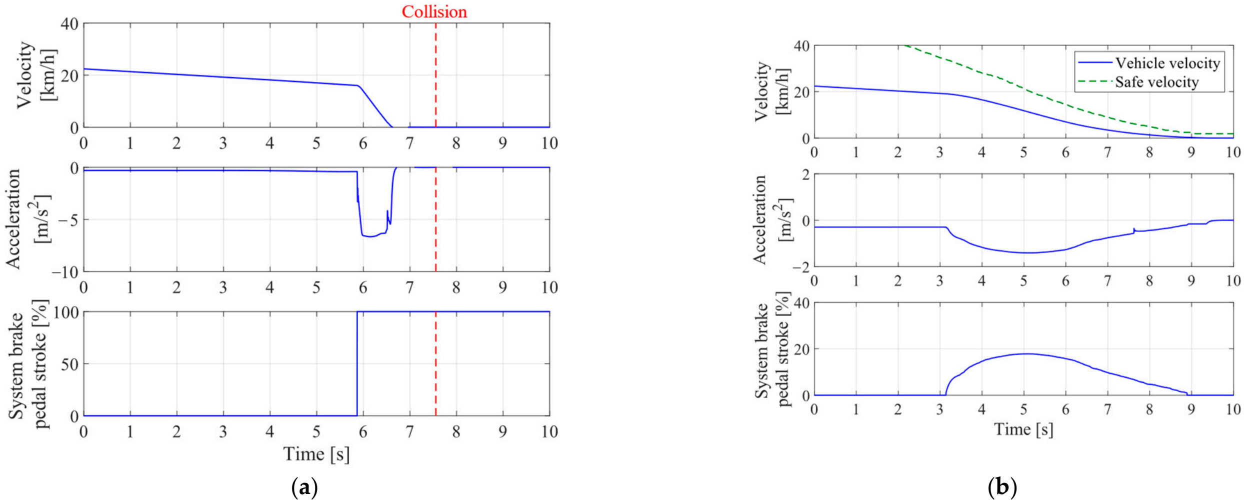

Figure 13. Time history of the ego vehicle in the simulation (V_{obj}= 50 km/h, D_{obj_offset} = 16 m). (**a**) AEBS; (**b**) PBS and AEBS.

To verify the degree of collision risk at the time instant the on-board sensor detected a darting out, the time to conflict area of the ego vehicle and the darting-out object was compared. Figure 14 shows a representative example of the time history of T_{ego_in}, T_{ego_out}, T_{obj_in}, and T_{obj_out} described in Section 4.1. In Figure 14, we extracted the simulation condition where collisions in neither the case of AEBS-equipped vehicle nor the case of PBS-AEBS-equipped vehicle occurred (V_{obj} = 40 km/h, D_{obj_offset} = 12 m). The black dotted vertical line indicates the time instant when the object was detected, and the red dotted vertical line indicates the time instant when the system was activated in Figure 14. In addition, the blue shaded area corresponds to the time zone in which the ego vehicle body will occupy the space in the conflict area in the future, and the red shaded area corresponds to the time zone in the case of the darting-out object. If these two time zones overlap, it means that a collision will occur at a certain horizon time if both vehicles maintain their current velocity. Figure 14a shows that the time zones in which the ego vehicle and object occupy the conflict area overlapped when the on-board sensor detected the object. Therefore, although AEBS was able to avoid a collision under this driving condition, the collision risk was high, and it was near-miss a situation. On the other hand, Figure 14b shows that PBS started decelerating 2.7 s before the darting-out detection, moving to a state in which the time zones of the conflict area occupancy did not overlap. As a result, since the occupied time zones no longer overlapped ($T_{ego\_in} - T_{obj\_out}$ = 0) at the time of darting-out detection, it was not considered to be a near-miss situation.

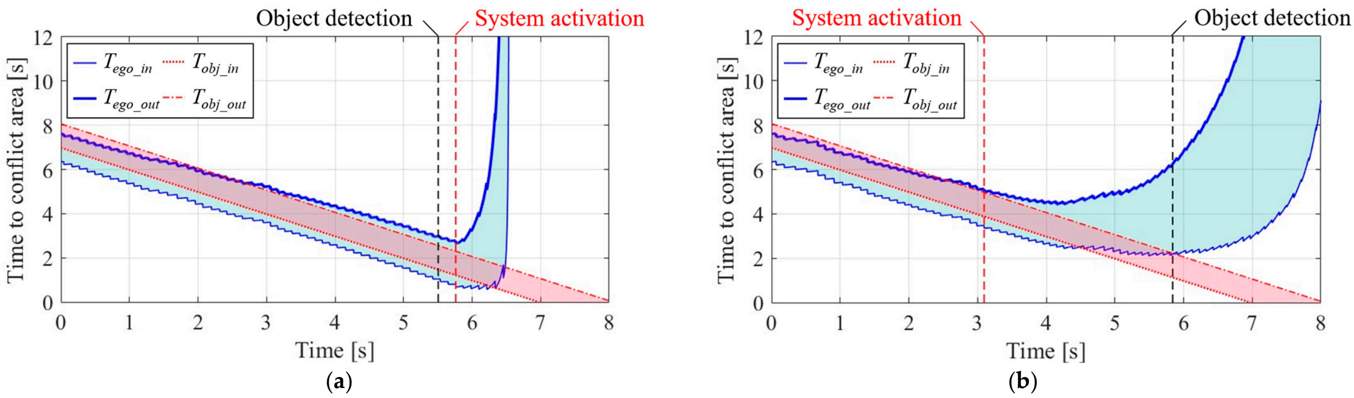

Figure 14. Time history of T_{ego_in}, T_{ego_out}, T_{obj_in}, and T_{obj_out} (V_{obj} = 40 km/h, D_{obj_offset} = 12 m). (**a**) AEBS; (**b**) PBS and AEBS.

To analyze the time margin for deceleration at the time of darting-out detection, the Safety Cushion Time (SCT) as an index of situational risk assessment proposed by Saito et al. [30] was calculated. SCT is the time margin for the driver to avoid a collision when an object crosses the road from a blind area in front of the ego vehicle. SCT at the time of object detection is expressed by the following equation:

$$SCT = \frac{\left\{ D_{ego\_in}(t^*) + \frac{V_{ego}(t^*)^2}{2a_{max}} \right\}}{V_{ego}(t^*)} - \tau \tag{10}$$

where t^* is the time when the object is detected, a_{max} (= -6 m/s^2) is the maximum acceleration achievable during the avoidance action phase, and τ (=0.25 s) is the required time for the vehicle to decelerate after the driver initiates the brake action. SCT results of the simulation are shown in Figure 15. The vehicle equipped with PBS decelerated without using AEBS under all simulation conditions. Figure 15 shows that all the SCT for the vehicle equipped with AEBS were lower than 1.2 s, whereas those with PBS were higher than 1.6 s. Therefore, PBS provided a larger time margin for collision avoidance than AEBS. Next, SCT was classified into three criticality levels according to the previous study [30]. The classification method of criticality level and the percentage results for each level are shown in Table 2. Most of the situations for vehicles equipped with AEBS were near-miss situations, as 98.6% of cases were classified as high-level critical events. On the other hand, the criticality level of PBS was split between middle level and low level, and there were no high-level events. Therefore, compared to the case of AEBS only, additional braking control by the proposed PBS was able to significantly reduce the near-miss situations (critical situations) when darting-out was detected.

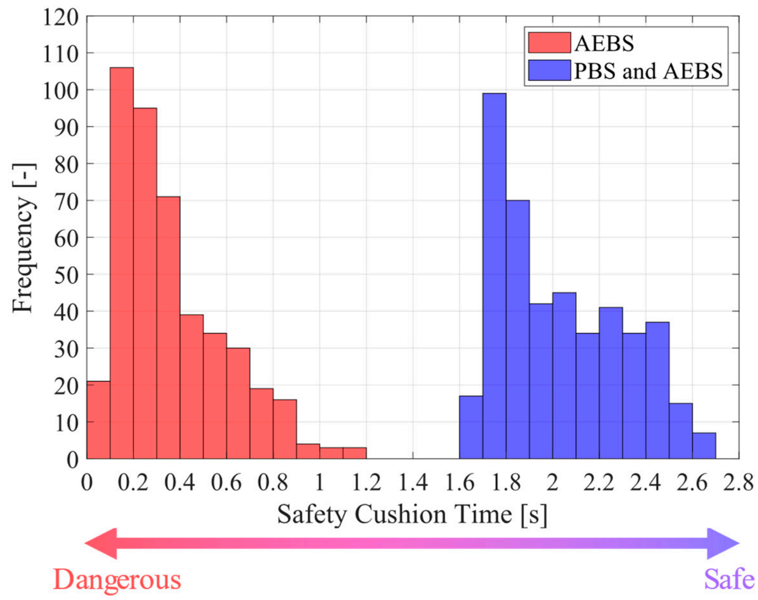

Figure 15. Comparison of Safety Cushion Time as a risk index.

Table 2. Percentage of criticality level.

Criticality Level	AEBS	PBS and AEBS
High level (SCT < 1 s)	98.6%	0%
Middle level (1 s ≤ SCT ≤ 2 s)	1.4%	51.7%

Next, Figure 16a,b show the results of the collision/non-collision as well as the DCPA for each driving condition. The smaller the value of DCPA, the higher the collision risk.

The magnitude of the DCPA was indicated by red-to-white gradation shading. In addition, the red cells with a black dot indicate collision cases and the blue cells indicate the cases where the ego vehicle turns right before coming into contact with the darting-out object. Figure 16a,b show that the PBS reduced the number of collision cases from 143 to 0 compared to AEBS. In Figure 16a, there were 133 cases where the DCPA was less than 1 m for vehicles equipped with AEBS, excluding collision cases. Furthermore, in some cases, the DCPA was less than 20 cm. These results indicate that although no collisions occurred in the simulation cases, the safety margin was small, and the collision risk was considered to be high. On the other hand, with the additional braking by the proposed PBS, the DCPA could be extended to exceed 1 m in all simulation cases. Therefore, it can be concluded that PBS was able to calculate a stop position with a low risk of collision and then stop the controlled vehicle in a safe space.

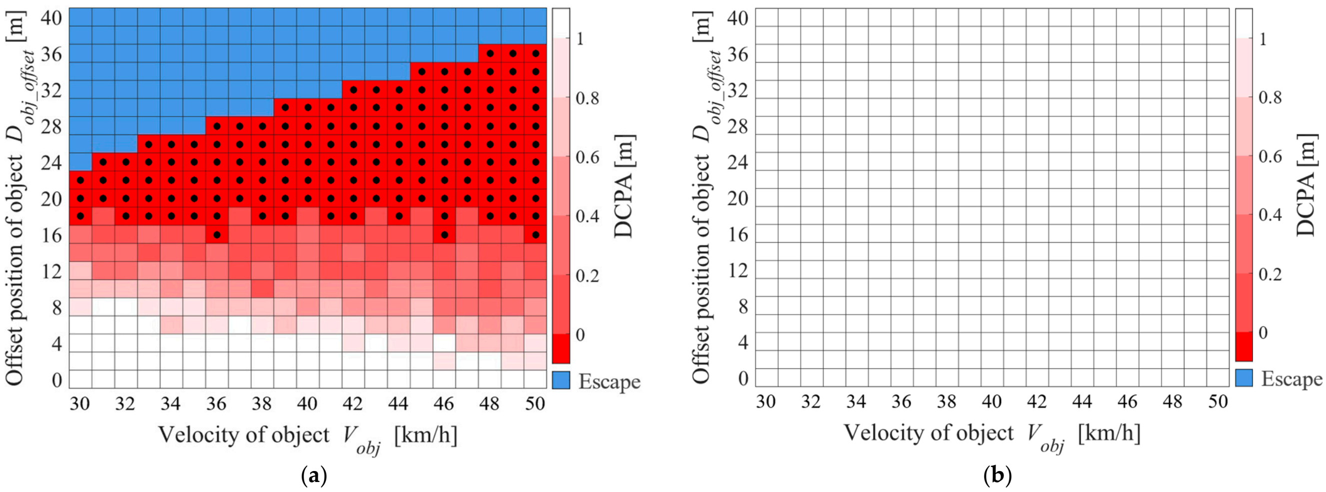

Figure 16. Collision case and distance to the closest point of approach (DCPA) heat map. (**a**) AEBS (Black dots indicate the collision cases); (**b**) PBS and AEBS.

To compare the previous system with the new system, simulations were performed in representative cases. The previous system PBS_f was reproduced with a_b = 7.85 m/s^2 and the on-board sensor mounted at the middle of the front end of the vehicle, based on the theory proposed by Fujinami et al. [24]. Figure 17 shows the simulation result of the previous system (PBS_f and AEBS) and the new system (PBS and AEBS). As shown in Figure 17, the previous system decelerated with AEBS, but the collision occurred because the ego vehicle entered the object's driving corridor, i.e., the stop position of the ego vehicle is inside the predicted conflict area. On the other hand, the new system stopped before entering the conflict area and avoided a collision. Furthermore, as shown in Figure 17a, since the previous system decelerated rapidly at -8 m/s^2, there was a rear-end collision risk if the following vehicle could not brake at the same level as the ego vehicle in time. On the other hand, as shown in Figure 17b, the new system decelerated more slowly at accelerations higher than -2 m/s^2. Therefore, the new system could reduce the rear-end collision risk, since the following vehicle would not need to brake suddenly.

As described in Section 2.2, this system is designed to avoid collisions with vehicles darting out at the determined virtual velocity V_{vir} or under. On the other hand, a study of naturalistic driving data at intersections in Japan and Germany by Thal et al. shows that darting-out vehicles exceed the speed limit at a certain rate [31]. Therefore, we simulated the case of darting out at a higher velocity than the assumed virtual velocity V_{vir}. Figure 18 shows the results of maximum deceleration with PBS and AEBS. The assumed virtual velocity V_{vir} was 50 km/h, and the velocity of object V_{obj} varied from 50 km to 70 km/h. The magnitude of deceleration was indicated by blue-to-white shading. In Figure 18, the dark blue cells with deceleration under -6 m/s^2 indicate that AEBS was activated, the light blue cells with deceleration between $-4\ \mathrm{m/s^2}$ and $-1\ \mathrm{m/s^2}$ indicate mild deceleration by PBS, and the white cells between $0\ \mathrm{m/s^2}$ and $-1\ \mathrm{m/s^2}$ indicate that the ego vehicle escaped the intersection before coming into contact with the object. Figure 18 shows that AEBS was activated for cases where darting-out occurs at 53 km/h or higher. In addition, the number of AEBS activation cases increased as the object velocity became higher than V_{vir}. On the other hand, even at velocities exceeding V_{vir}, collisions were avoided in all cases by activating PBS or AEBS. These results suggest that this system has a high possibility of avoiding a collision even when a darting-out occurs at a velocity exceeding prediction. However, it was also confirmed that in some cases, the system was not able to achieve its design goal of mild deceleration without emergency braking. This is because the system predicted that there was no dilemma zone and determined that the ego vehicle could escape, but the detected velocity was higher than predicted. As a result, the ego vehicle was in a dilemma zone and it was necessary to activate the AEBS to stop in time. This result shows that it is necessary to accurately predict and set the parameters of the logical scenario such as the determined virtual velocity of the oncoming objects V_{vir} in this system.

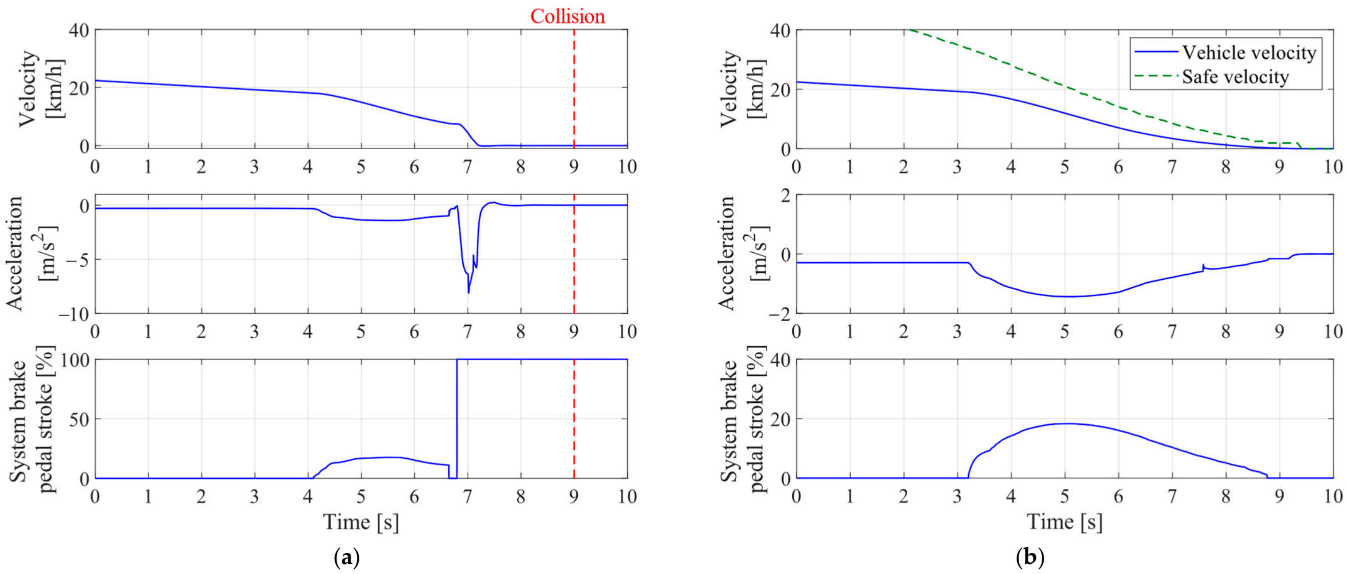

Figure 17. Time history of the ego vehicle in the simulation (V_{obj}= 50 km/h, D_{obj_offset} = 40 m). (**a**) Previous system (PBS_f and AEBS); (**b**) new system (PBS and AEBS).

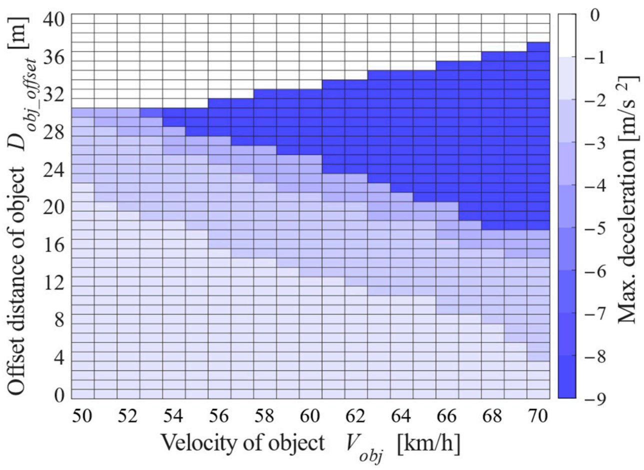

Figure 18. Maximum deceleration in cases of darting out at a higher-than-expected velocity.

5. Conclusions

This paper described the collision avoidance system by proactive braking control with an oncoming vehicle that darts out under occluded vision when turning right at an intersection in left-hand traffic. We proposed a proactive driver assistance system that avoids the right-turn dilemma zone, with the assumption that the vehicle under test (VUT) uses only on-board sensors without infrastructure coordination facilities. The right-turn dilemma zone is defined as the region of the vehicle's hazardous speed where the vehicle cannot avoid collision safely when a vehicle darts out suddenly. The proposed proactive braking system provides braking assistance to avoid the right-turn dilemma zone. The simulation study using a right-turn across a path scenario with various conditions of the position of the oncoming vehicle and the darting-out velocity of that vehicle reveals that the proactive braking control system is able to decelerate the vehicle in advance before a darting-out of oncoming vehicle occurs, and consequently stop the vehicle with mild deceleration without activating AEBS. In addition, we confirmed that the proactive braking control system effectively reduces the possibility of collisions and near-miss situations, using situational risk assessment such as Safety Cushion Time (SCT), when a darting out is detected, compared to the conventional AEBS. Comparison with the previous system described in [24] showed that the proposed system solved the problems of the previous system: rear-end collision risk due to emergency braking and certain conditions where collisions cannot be avoided.

Future research will focus on enhancing the performance of the control system to ensure its effectiveness in accident prevention. In particular, we will examine the effect of collision avoidance performance and the interaction between human driver and the braking control system due to variations in intersection geometry (e.g., the intersection size, the number of lanes, the angle of the intersection, etc.) through simulations.

Author Contributions: Conceptualization, S.A., Y.F. and P.R.; methodology, S.A., Y.F. and P.R.; validation, S.A.; data analysis and visualization, S.A., Y.F. and P.R.; discussion, S.A., Y.F. and P.R; writing—original draft preparation, S.A.; writing—review and editing, S.A., Y.F., P.R., and R.H. All authors have read and agreed to the published version of the manuscript.

Funding: This work was supported by JSPS Grant-in-Aid for Scientific Research(C) 21K03977 in coordination with Fund for the Promotion of Joint International Research 22KK0237.

Institutional Review Board Statement: Not applicable.

Informed Consent Statement: Not applicable.

Data Availability Statement: The raw data supporting the conclusions of this article will be made available by the authors on request.

Conflicts of Interest: The authors declare no conflicts of interest.

References

1. National Police Agency Traffic Bureau. *Status of Traffic Fatal Accident Occurrence and Status of Violation Control of Road Traffic Act in 2022*; Portal Site of Official Statistics of Japan: Tokyo, Japan, 2023; p. 33.
2. Institute for Traffic Accident Research and Data Analysis (ITARDA). Right turn traffic accidents in signalized Intersection. *ITARDA Inf.* **2012**, *95*, 4.
3. Sander, U. Opportunities and Limitations for Intersection Collision Intervention—A Study of Real World, Left Turn Across Path, Accidents. *Accid. Anal. Prev.* **2017**, *99*, 342–355. [CrossRef]
4. Sander, U.; Lubbe, N.; Pietzsch, S. Intersection AEB implementation strategies for left turn across path crashes. *Traffic Inj. Prev.* **2019**, *20*, S119–S125. [CrossRef] [PubMed]
5. Hillenbrand, J.; Spieker, A.M.; Kroschel, K. A multilevel collision mitigation approach -its situation assessment, decision making, and performance tradeoffs. *IEEE Trans. Intell. Transp. Syst.* **2006**, *7*, 528–540. [CrossRef]
6. Brännström, M.; Coelingh, E.; Sjöberg, J. Model-based threat assessment for avoiding arbitrary vehicle collisions. *IEEE Trans. Intell. Transp. Syst.* **2010**, *11*, 658–669. [CrossRef]
7. Brännström, M.; Sjöberg, J.; Helgesson, L.; Christiansson, M. A Real-time Implementation of an Intersection Collision Avoidance System. *IFAC Proc.* **2011**, *44*, 9794–9798. [CrossRef]

8. Nobukawa, K.; Gordon, T.J.; Barnes, M.A.; Goodsell, R.J. A comprehensive speed control model for human drivers with application to intersection left turns. In Proceedings of the 2011 American Control Conference, San Francisco, CA, USA, 29 June–1 July 2011; pp. 3065–3070. [CrossRef]
9. Brännström, M.; Sandblom, F.; Hammarstrand, L. A probabilistic framework for decision-making in collision avoidance systems. *IEEE Trans. Intell. Transp. Syst.* **2013**, *14*, 637–648. [CrossRef]
10. Yoshihira, M.; Watanabe, S.; Nishira, H.; Kishi, N. Developing an Autonomous Vehicle Control System for Intersections Using Obstacle/Blind Spot Detection Frames. *SAE Tech. Pap.* **2016**. [CrossRef]
11. Arikere, A.; Yang, D.; Klomp, M. Optimal motion control for collision avoidance at Left Turn Across Path/Opposite Direction intersection scenarios using electric propulsion. *Veh. Syst. Dyn.* **2019**, *57*, 637–664. [CrossRef]
12. Fors, V.; Olofsson, B.; Nielsen, L. Yaw-Moment Control At-the-Limit of Friction Using Individual Front-Wheel Steering and Four-Wheel Braking. In Proceedings of the 9th IFAC Symposium on Advances in Automotive Control, Orléans, France, 23–27 June 2019; Volume 52, pp. 458–464. [CrossRef]
13. Pierowicz, J.A. Intersection Collision Avoidance Using ITS Countermeasures. 2000. Available online: http://hdl.handle.net/2027/mdp.39015075257181 (accessed on 8 February 2024).
14. Misener, J.A. *Cooperative Intersection Collision Avoidance System (CICAS): Signalized Left Turn Assist and Traffic Signal Adaptation*; University of California: Berkeley, CA, USA, 2010; Report No.: UCB-ITS-PRR-2010-20; Available online: https://trid.trb.org/view.aspx?id=919887 (accessed on 8 February 2024).
15. Hafner, M.R.; Cunningham, D.; Caminiti, L.; Del Vecchioet, D. Cooperative collision avoidance at intersections: Algorithms and experiments. *IEEE Trans. Intell. Transp. Syst.* **2013**, *14*, 1162–1175. [CrossRef]
16. Nakamura, S.; Suganuma, H.; Kikuchi, K.; Homma, R. Effect Evaluation of Vehicle-Infrastructure Cooperative Right-Turn Collision Prevention System. *Trans. Soc. Automot. Eng. Jpn.* **2015**, *46*, 449–454. [CrossRef]
17. Hirose, T.; Ohtsuka, Y.; Gokan, M. *Activation Timing of a Collision Avoidance System with V2V Communication*; SAE Technical Paper 2017-01-0039; SAE: Warrendale, PA, USA, 2017. [CrossRef]
18. Yonekawa, T.; Murano, T.; Aga, M. Accident analysis on intersection right turning by using driving simulator. *Int. J. Veh. Saf. (IJVS)* **2014**, *7*, 17–36. [CrossRef]
19. Bärgman, J.; Smith, K.; Werneke, J. Quantifying drivers' comfort-zone and dread-zone boundaries in left turn across path/opposite direction (LTAP/OD) scenarios. *Transp. Res. Part F Traffic Psychol. Behav.* **2015**, *35*, 170–184. [CrossRef]
20. Wang, X.; Zhao, D.; Peng, H.; LeBlanc, D.J. Analysis of unprotected intersection left-turn conflicts based on naturalistic driving data. In Proceedings of the IEEE Intelligent Vehicles Symposium (IV), Los Angeles, CA, USA, 11–14 June 2017; pp. 218–223. [CrossRef]
21. Appiah, J.; King, F.A.; Fontaine, M.D.; Cottrell, B.H. Left turn crash risk analysis: Development of a microsimulation modeling approach. *Accid. Anal. Prev.* **2020**, *144*, 105591. [CrossRef]
22. Kusakari, Y.; Oikawa, S.; Matsui, Y.; Kubota, N. Effect of Human–Machine Interface of a Vehicle on Right-Turn Maneuver at Intersections using a Driving Simulator. In Proceedings of the IEEE International Conference on Systems, Man, and Cybernetics (SMC), Melbourne, Australia, 17–20 October 2021; pp. 1607–1612. [CrossRef]
23. Zafian, T.; Ryan, A.; Agrawal, R.; Samuel, S.; Knodler, M. Using SHRP2 NDS data to examine infrastructure and other factors contributing to older driver crashes during left turns at signalized intersections. *Accid. Anal. Prev.* **2021**, *156*, 106141. [CrossRef] [PubMed]
24. Fujinami, Y.; Raksincharoensak, P.; Ulbricht, D.; Adomat, R. Risk Predictive Driver Assistance System for Collision Avoidance in Intersection Right Turns. *J. Robot. Mechatron.* **2018**, *30*, 15–23. [CrossRef]
25. Fujinami, Y.; Raksincharoensak, P.; Arita, S.; Kato, R. Experimental Validation on Intersection Turning Trajectory Prediction Method for Advanced Driver Assistance System Based on Triclothoidal Curves. *Appl. Sci.* **2021**, *11*, 5900. [CrossRef]
26. Gazis, D.; Herman, R.; Maradudin, A. The problem of the amber signal light in traffic flow. *Oper. Res.* **1960**, *8*, 112–132. [CrossRef]
27. Allen, B.L.; Shin, B.T.; Copper, P.J. Analysis of traffic conflicts and collisions. *Transp. Res. Rec.* **1978**, *667*, 67–74.
28. Perri, G.; Vaiana, R. Road Safety Management of Uncontrolled Access Points: Design Criteria and Insights into Risk Factors. *Appl. Sci.* **2022**, *12*, 12661. [CrossRef]
29. Scanlon, J.M.; Sherony, R.; Gabler, H.C. Earliest Sensor Detection Opportunity for Left Turn across Path Opposite Direction Crashes. *IEEE Trans. Intell. Veh.* **2017**, *2*, 62–70. [CrossRef]
30. Saito, Y.; Raksincharoensak, P.; Inoue, H.; EI-Haji, M.; Freudenmann, T. Context-Sensitive Hazard Anticipation Based on Driver Behavior Analysis and Cause-and-Effect Chain Study. In Proceedings of the 14th International Symposium on Advanced Vehicle Control (AVEC'18), Beijing, China, 16–20 July 2018; pp. 1–6.
31. Thal, S.; Wallis, P.; Henze, R.; Hasegawa, R.; Teranishi, S.; Nakamura, H.; Kitajima, S.; Abe, G. Comparison of German and Japanese Urban Intersection Data for Internationally Harmonized Test Procedures. In Proceedings of the 7th International Symposium on Future Active Safety Technology towards zero-traffic-accidents (FAST-zero'23), Kanazawa, Japan, 8–11 November 2023; pp. 1–6.